Paper No. 493. (quote when citing this article)
Eleventh World Conference on Earthquake Engineering
ISBN: 0 08 042822 3

ACTIVE CONTROL EFFECT OF A MODEL STRUCTURE BY MASS DRIVER SYSTEM

Masaaki YOSHIKAWA [1], Kenzo TOKI [2], Tadanobu SATO [3] and Teruo TAKEUCHI [4]

[1 & 4] Department of Civil Engineering, Kochi National College of Technology
Otsu, Monobe, Nangoku-shi, Kochi-ken JAPAN 783
[2] Department Civil Engineering, Kyoto University
[3] Disaster Prevention Research Institute, Kyoto University

ABSTRACT

The new control algorithm has been introduced to a model eight-story building to demonstrate reduction of vibrations caused by medium earthquakes. As forced vibration tests, sinusoidal excitation to identify the dynamic characteristics of the model structure, non-stationary random wave excitation tests using filtered white noise wave as well as EL Centro NS seismic wave were carried out on a 4m by 4m shaking table. An active dynamic mass damping system installed at the top floor of model structure driven by an AC servomotor through a ball screw was developed. The optimization of the controller is performed taking into account the dynamic characteristics of AMD with the driving mass of 1 kgf By carrying out digital computer-controlled tests and numerical calculations using the model frame structure, we have obtained that the proposed open-closed control algorithms could perform good control efficiencies and there is an ample possibility for them to be used for seismic response control of actual structures.

KEYWORDS

Seismic response control ; AC servomotor ; model shaking table test ; active mass driver ; closed-open-loop optimal control algorithm

INTRODUCTION

The rapid development of such closely linked new technology as sensing units, actuators, computers, microprocessors, etc. has also contributed to the feasibility of implementing structural control. The first full scale applications of the active structural control in Japan have been realized by (Kajima, 1991 and other Japanese general constructions, 1994). Many of the control algorithms used to calculate the control forces, proposed for the control of civil structures, have merely been adopted from optimal regulator problems. The closed-loop control algorithms are the most widely used for earthquake-excited structures. This is a special case in which the control force is regulated by the response state vector and the Riccati matrix. It has been pointed out that because external excitation usually is ignored in the derivation of the Riccati equation, the closed-loop control law is not truly optimal. If the excitation term is included in the Riccati equation, its solution requires a priori knowledge of the loading history. This generally is not possible for excitations such as earthquakes.

To overcome this difficulty we proposed a new instantaneous closed-open-loop control law which takes

into account the energy of the earthquake motion to the structure's input (Sato et al., 1990). A time-dependent performance index similar to that defined by (Yang, 1987) was used to obtained the control vector. On the basis of Yang's work, a series of theoretical and experimental studies in which used a new instantaneous closed-open-loop control algorithm of active mass drivers have been made and reported by (Toki et al., 1990, Sato et al., 1994). The minimization of a newly defined objective function results in three control algorithms with different control efficiencies. The main purpose of this study is to examine the efficiency of our proposed control algorithms in the experimental studies of an eight-story model structure.

THEORETICAL BACKGROUND FOR THE CONTROL ALGORITHM

Modal Analysis

A structure that is idealized by an n-degree of freedom system with one active mas driver (AMD) on the top floor is subjected to one-dimensional earthquake ground acceleration, $\ddot{X}_0(t)$.

$$M\ddot{x}(t) + C\dot{x}(t) + Kx(t) = -m\ddot{X}_0(t) + Hu(t) \tag{1}$$

in which M, C, K respectively are the $(n \times n)$ mass, damping and stiffness matrices, x is the n-dimensional relative displacement of the structure to the ground, u the r-dimensional control vector, H an n-dimensional vector with the component $\{1, 0, \cdots, 0\}^T$ because an active mass driving type controller is placed on the top floor, and m an n-dimensional mass vector expressed as $\{m_1 + m_d, m_2, \cdots, m_n\}$, in which m_d is the mass of the AMD. The control force used in the experiment (Toki et al., 1994) is written

$$u(t) = \{F_{BV}\}\{\dot{x}\} + F_f \ddot{X}_0 \tag{2}$$

in which $\{F_{BV}\}$ is the feedback gain for the relative velocity of the structure, and F_f, the feedforward gain for the input motion. The feedback gain for relative displacement is assumed to be zero. Transformation to the generalized coordinates using the eigen function expansions

$$\{x\} = [\Phi]\{q\} \tag{3}$$

in which $\{q\}$ is the vector of the model amplitudes and $[\Phi]$ the matrix of normalized mode shapes, leads to n differential equations;

$$\{\ddot{q}\} + [\zeta]\{\dot{q}\} + [\Omega]\{q\} = -[\Phi]^T\{m\}\ddot{X}_0 + [\Phi]^T Hu(t) \tag{4}$$

in which $[\zeta]$ and $[\Omega]$ are the diagonal matrix with the respective components $2h_i\omega_i$ and ω_i^2. Assuming that only a certain ordered number of modes are to be controlled, the modal amplitudes are partitioned into controlled modes, Φ_c, and residual modes, Φ_r, as follows:

$$[\Phi] = [\Phi_c \mid \Phi_r] \tag{5}$$

The equation of controlled and residual modes is written

$$\{\ddot{q}_c\} + [\zeta_c]\{\dot{q}_c\} + [\Omega_c]\{q_c\} = -[\Phi_c]^T\{m\}\ddot{X}_0 + [\Phi_c]^T\{H\}u \tag{6}$$

$$\{\ddot{q}_r\} + [\zeta_r]\{\dot{q}_r\} + [\Omega_r]\{q_r\} = -[\Phi_r]^T\{m\}\ddot{X}_0 + [\Phi_r]^T\{H\}u \tag{7}$$

Open-loop control

To clarify the effect of the feedforward term, we examine the case in which the control force is generated by the feedforward term:

$$u = F_f \ddot{X}_0 \tag{8}$$

Substituting Eq. (8) into Eq. (4) the equation of motion for the ith mode is given by

$$\ddot{q}_i + \zeta_i \dot{q}_i + \Omega_i q_i = - \{\phi_i\}^T \{m\} \ddot{X}_0 + \{\phi_i\}^T \{H\} F_i \ddot{X}_0 \quad (9)$$

Obviously, the feedforward term in the control force offsets the excitation term of the i th mode if F_i is chosen as follows:

$$F_i = \frac{\{\phi_i\}^T \{m\}}{\phi_i^1} \quad (10)$$

in which ϕ_i^1 is the first component of vector $\{\phi_i\}$. Although the excitation term becomes zero for the i th mode when using the feedforward gain defined in Eq.(10), its affects the excitation term of other modes. The equation motion of the k th mode yields

$$\ddot{q}_k + \zeta_k \dot{q}_k + \Omega_k q_k = - (\{\phi_k\}^T \{m\} - \frac{\phi_k^1}{\phi_i^1} \{\phi_i\}^T \{m\}) \ddot{X}_0, \ (k \neq i) \quad (11)$$

The participation factor of the k th mode changes from $\{\phi_k\}^T \{m\}$ to

$$\{\phi_k\}^T \{m\} - \frac{\phi_k^1}{\phi_i^1} \{\phi_i\}^T \{m\} \quad (12)$$

The second term of this participation factor is regarded to be the leaking effect of the control force to the other mode when the i th mode's excitation is perfectly offset.

EXPERIMENTAL PROCEDURE

Dynamic property of an eight-story model structure

To demonstrate the application of the algorithm, an eight-story model building shown in Fig. 1 was used in the seismic response control experiment. An active mass driver controller was installed on the top floor . The eight-story structure which can be reduced to a shearing beam model with 8 degrees of freedom is made of floors with steel frames and flat springs with columns with a total weight of 1.0 tonf to vibrate in a shear-type mode. The dynamic characteristics of this model structure, the first floor being the level at which seismic motion is input, have been estimated from the results of several shaking table tests. We used sinusoidal excitation and non-stationary random wave excitation tests that used filtered white noise wave as wall as the EL Centro NS seismic wave. The white noise earthquake motion with the El centro NS phase because the control effect depends on the characteristics of the input motions is simulated. The frequency response curve shown in Fig. 2 was obtained from a sinusoidal excitation test with a constant amplitude of 20 cm/sec ^{2} and a sweeping frequency of 0 to 18 Hz. The identified natural frequency and damping ratio of each mode are given in Table 1. The calculated frequency response and phase change curves based on the identified dynamic characteristics are shown by the solid line in Fig. 3.

Feedback and feedforward gains

The feedback and feedforward gains defined in Eq. (2) expressed for this model structure are (Sato et al., 1994)

$$\{F_{BV}\} = - \frac{\Delta t}{4r} (\{m^{-1}\}\{H\})^T [Q_{21}^T + Q_{21}], \quad F_t = \frac{\Delta t^2 \alpha}{8} \frac{}{r} \quad (13)$$

In closed-loop control the control force is determined by the value of $r^{-1} Q$ as given in Eq. (13). To determine the appropriate weighting matrices, Q, in which the order of matrices Q_{ij} is (8 × 8), we use the characteristics that the submatrices Q_{11} and Q_{12} do not contribute to the active forces. Q_{11} and Q_{12} are designated as zero even though Q must be a positive definite symmetric matrix. When the feedback of relative displacement is not taken into account, Q_{22} must be the zero matrix. The appropriate assignment of the elements of Q_{21} to obtain maximum control efficiency was not

investigated because it requires a two-stage optimization technique that is beyond the scope of the research reported here. Therefore the number of non-zero elements that can be defined independently is eight, and the following formula of matrix Q_{21} is sufficient to control the AMD system.

$$Q_{21} = \theta \cdot \begin{bmatrix} \theta_1 & \theta_2 \cdots \theta_8 \\ \theta_2 & \\ \vdots & \\ \cdot & [0] \\ \theta_8 & \end{bmatrix} \tag{14}$$

We assigned the following values to the ratio θ_i / r on the basis of results of several trials to obtain the most stable control performance by numerical simulations (Sato et al., 1994);

$\theta_1 / r = 1.0,\ \theta_2 / r = \theta_3 / r = 1.0,\ \theta_4 / r = \theta_5 / r = 0.5,\ \theta_6 / r = \theta_7 / r = \theta_8 / r = 0.05$

In the open-loop control, the control force is defined by Eq. (8), in which the feedforward gain F_I is a function of α / r. The optimal value of α / r for control of the i th mode vibration is defined by substituting Eq. (10).

$$(\alpha / r)_i = \frac{8}{\Delta t^2} \frac{\{\phi_i\}^T \{m\}}{\phi_i^T} \tag{15}$$

The value of α / r that offsets the seismic excitation term of each vibration mode is given in Table 2.

Control signal of AMD system

The configuration of the pickups ,the explanation of the digital signal processing, and the control signal flow are figured schematically in Fig. 4. The control force generated by a mass driver system placed on the top floor of the structure is

$$u = - m_d \ddot{x}_d \tag{16}$$

in which m_d is the mass of the driver and x_d the relative displacement of the driving mass to the top floor. The dynamic characteristics of the AC servomotor is assumed to be expressed by the first order delay elements as

$$Y^* = T \ddot{x}_d + \dot{x}_d \tag{17}$$

in which Y^* is the control signal of the AC servomotor, and T is the time constant. The control signal to drive the AC servomotor is expressed as a function of the modal displacements and modal velocities of the control modes, and input motion (Toki et al., 1994)

$$Y^* = -\frac{T}{m_d} \{\{F_{BV}\}[\Phi_c](\dot{q}_c + \frac{q_c}{T}) + F_I (\ddot{X}_0 + \frac{X_0}{T})\} \tag{18}$$

The modal states that appear in Eq. (18) are estimated from the output of discrete sensors at different locations in the building as follows:

$$\{q_c\} = [\Phi_c]^{-1} \{x_0\},\quad \{\dot{q}_c\} = [\Phi_c]^{-1} \{\dot{x}_0\} \tag{19}$$

in which x_0 and $\dot{x}_0$ respectively are the observed displacement and velocity vectors of the structure. Fig. 5 shows the dynamic characteristics of the AC servomotor used to generate the control force. The time constant in Eq. (17) is obtained to be 0.0015 from this figure.

RESULTS OF EXPERIMENTS

The control signal used to drive the active mass is a monotonous increasing function of θ and α / r, as seen from Eqs.(18) and (19). The control force increases as the values of these two parameters increase. We compared the experimental time histories of the structural response and control signal with the

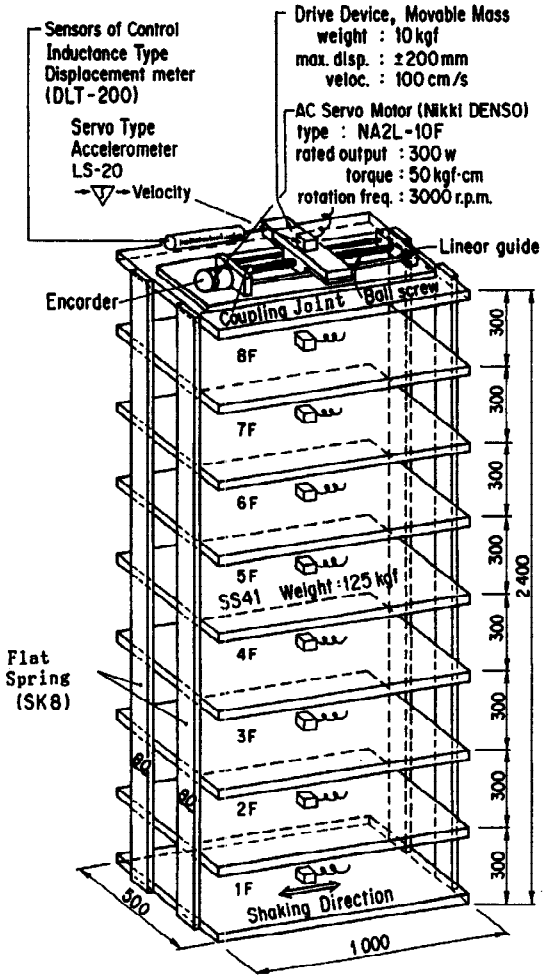

Fig. 1 Multistory building model with control system

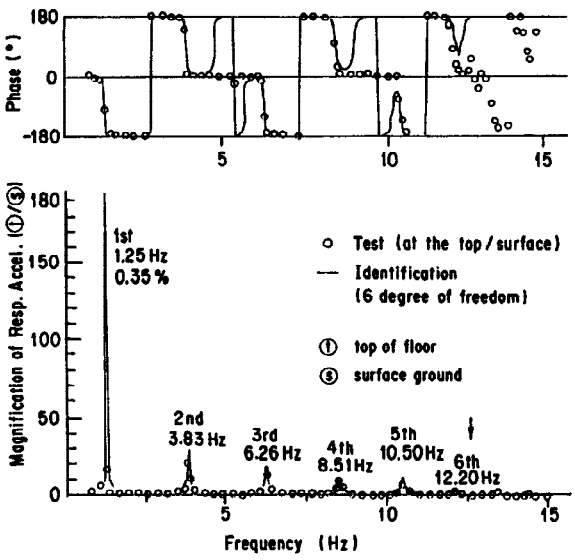

Fig. 3 Curve fit of identification

Table 1 Dynamic characteristics of 8 story model

	Mode	1	2	3	4	5	6	7	8
T	Natural Frequency (Hz)	1.25	3.72	6.19	8.55	10.47	12.24	13.42	14.30
I	Natural Frequency (Hz)	1.25	3.83	6.26	8.51	10.50	12.20	—	—
	Damping Ratio (%)	0.35	0.56	0.56	0.58	0.54	0.52	—	—

T : Test Result
I : Identification of Modal Constant from Resonance Curve

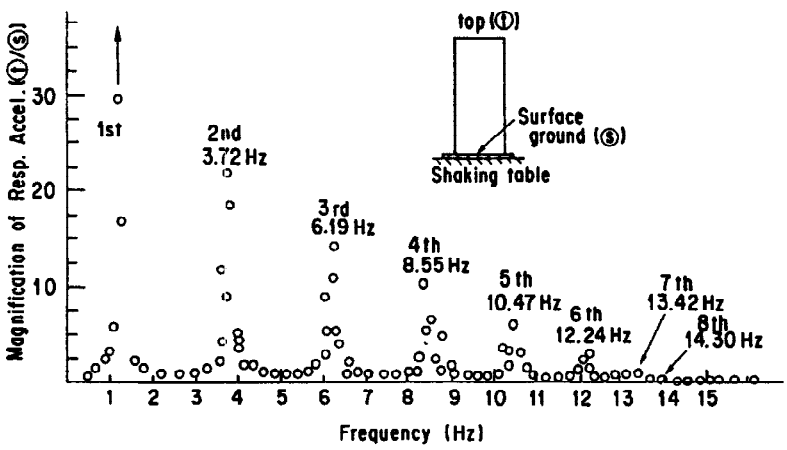

Fig. 2 Frequency response curve by continuous swept motion (20cm/s ^{2})

Table 2 α / r value offsetting the excitation term of each mode

Mode No.	α / r
1	56.6
2	-19.5
3	12.6
4	-10.0
5	8.6
6	-7.9
7	7.5
8	-7.3

analytical histories for the cases of a without control, a closed-loop control with a value of $\theta /r=10^{-5}$, an open-loop control with a value of $\alpha /r=27$, a closed -open-loop with a value of $\alpha /r=15$ and $\theta /r=10^{-6}$ respectively (Toki et al., 1994). The structural response obtained experimentally is slightly larger than that obtained analytically, but the overall tendencies agree well.

The relation between α /r and the maximum response of the top floor is shown i Fig. 6. Until the α /r value reaches the optimal value for offsetting the first mode response, as α /r increases the maximum response decreases to the minimum value then increases. If we assume a single degree of freedom system with the first mode characteristics, the maximum response must be zero at $\alpha /r=56.6$. In Fig. 6 the maximum response dose not reach zero because of the leaking effect. These cases are investigated to compare the control efficiencies of the newly proposed closed-open-loop algorithm; the open-loop control

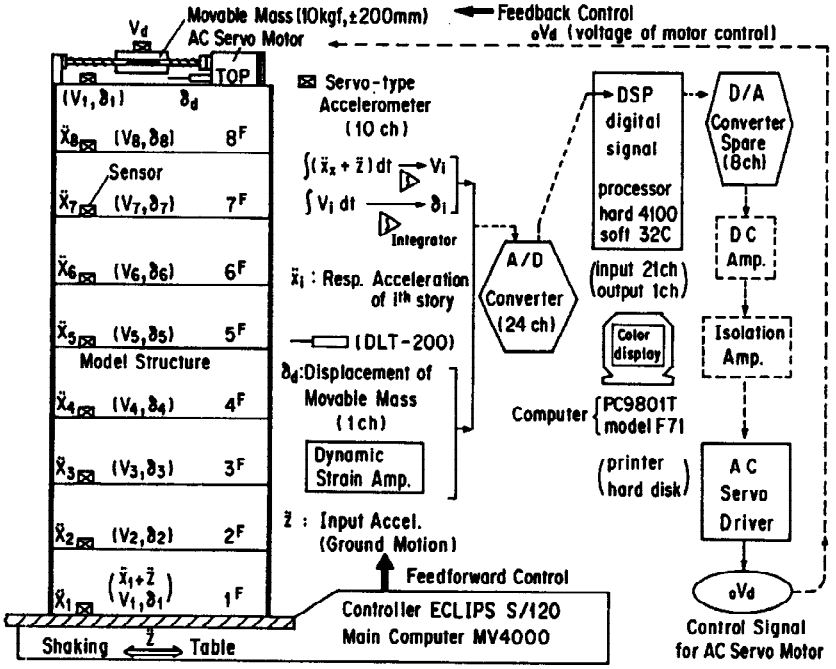

Fig. 4 Schematic of control system

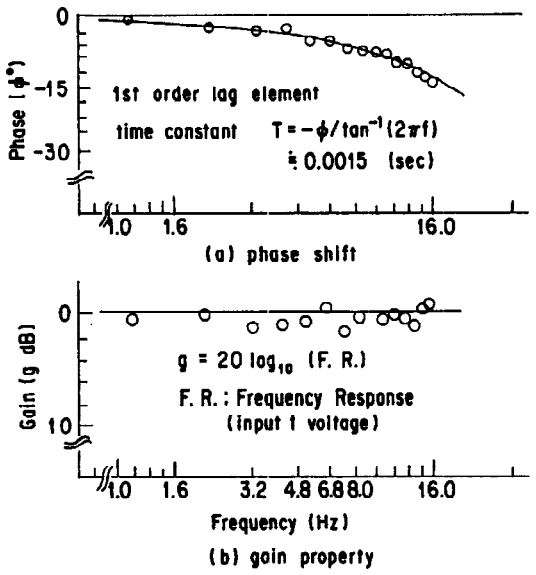

Fig. 5 Time constant of AC servomotor

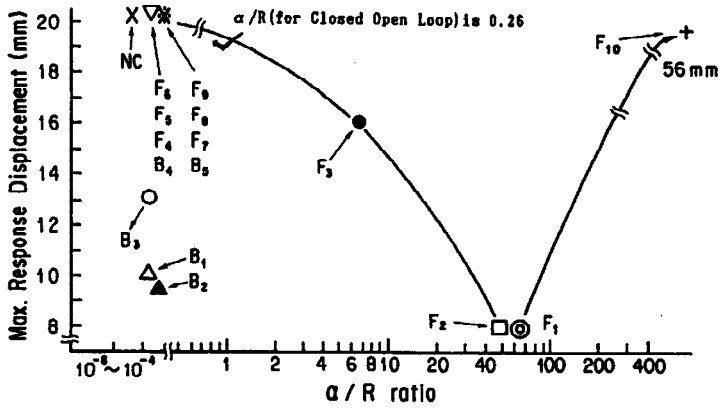

Fig. 6 Relationship between α /R and max. resp. displacement.

obtained by inserting $\theta = 0$ and increasing α / r from zero; the closed-loop control ($\alpha / r = 0$ and θ being increased); and the closed-open-loop control. In the case of the closed-open control, the effect of the closed-loop control depends on the parameter θ . The parameter θ is fixed of 5×10^{-6}, because the effect of closed-loop control is larger than that of the open-loop. After several trial and error searches of digital filters to increase the efficiency to the open-loop control algorithm, we found the band rejection filter that gave the best control performance to minimize the leaking effect of the control force. This band rejection filter is designed to cut off the frequency components of earthquake motion around the second mode natural frequency. This works well for reducing the leaking effect of the control force from the first to the second structural mode (Sato et al., 1994). Fig. 7 shows the theoretical results of the time history of the top floor response for three cases obtained by using the closed-loop, the open-loop and the closed-open-loop algorithm when a maximum control signal of 80 cm/sec is applied. The response time histories represent the characteristics of the control algorithms. The closed-loop control algorithm well reduces the structural response caused by the free vibration, but it is difficult to reduce the structural response caused by impulse type input motion. The open-loop control algorithm has the reverse characteristics. The combined control algorithm is expected to give suitable control performance for a variety of input time histories. The comparison of the experimental and theoretical results for three cases are shown in Fig. 8 as the control performance index. In the higher control signal range (from 50 to 100 cm/sec) of the control performance curve, the open-loop control algorithm gives a control efficiency about ten percent higher than that of the closed-loop algorithm in the theoretical results. For the closed-open -loop control, the experimental results show a good performance level.

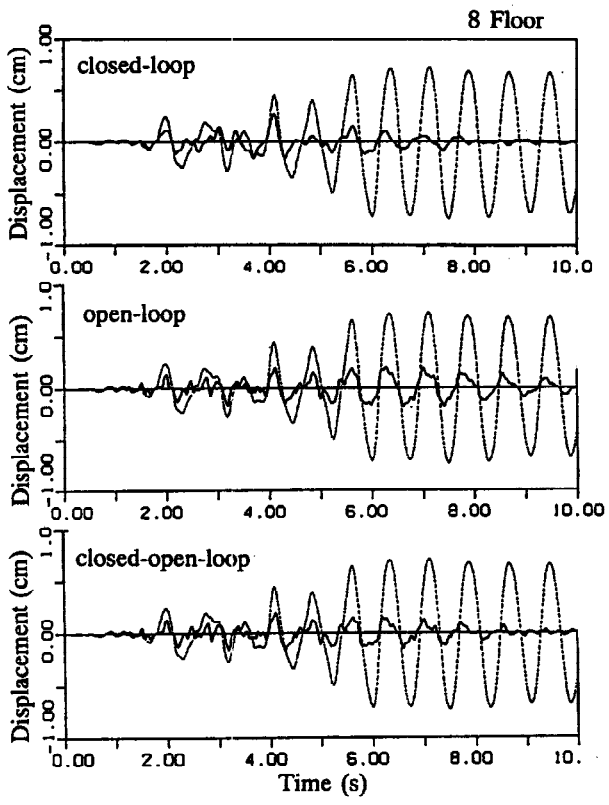

Fig. 7 Time histories of the top floor response simulated using different control algorithms

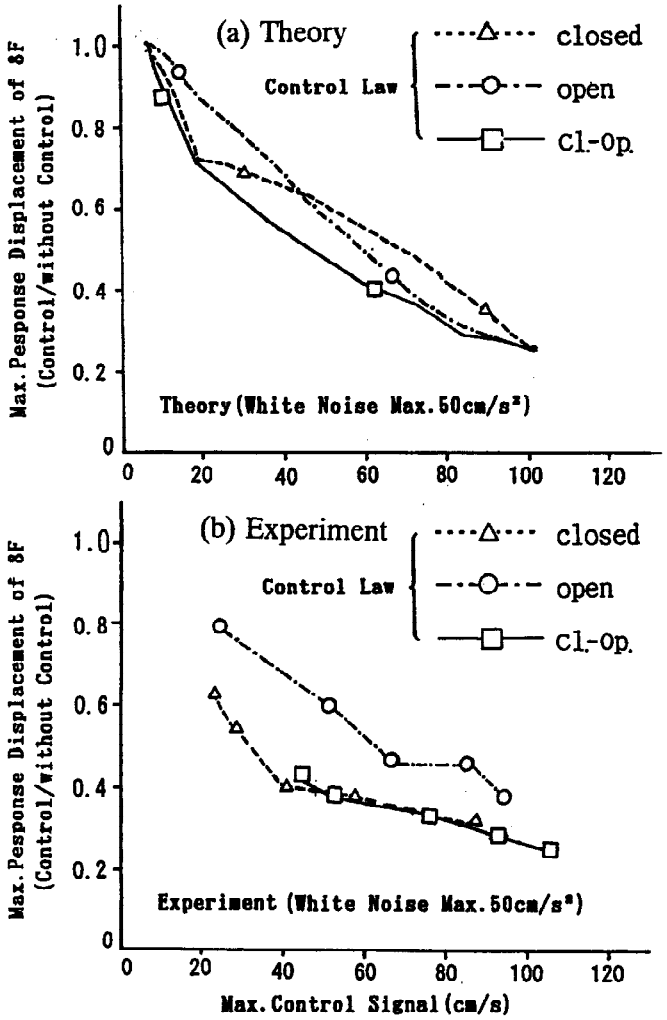

Fig. 8 Relationship between control signal and max. resp. displacement

CONCLUDING REMARKS

We have developed a new closed-open-loop active control algorithm and investigated the efficiency of our proposed control algorithm. The principle results of digital computer-controlled tests and numerical calculations using the model frame structure are summarized as follows:

(1) Effects of the control parameters on the system's response are expressed by two independent variables. One controls the level of feedback, the other reflects the level of input excitation. For a given structural system we found that there are appropriate control parameters to maximize the control efficiencies. From the modal control algorithm, we derived the optimal feedforward gain to offset the excitation term.

(2) Results of the experimental studies done to examine the applicability of the developed optimal control algorithm to an active mass driver system driven by an AC servomotor showed that the proposed closed-open-loop control algorithm gave better control efficiencies than the closed-loop control algorithm and that the seismic response control of actual structures is possible by using them.

ACKNOWLEDGEMENTS

The authors express sincere thanks and appreciation to Tsukuba Research Institute of Okumura Corp. for their assistance in performance of the tests for proving.

REFERENCES

Ohzca, S., Kawai, N. and Shimada, I. (1994). Development and verification of Active/Passive Mass Damper. Proc. of the 1st World Conf. on Structural Control, Los Angeles

Kobori, T., Koshika, N., Yamada, K. and Ikeda Y. (1991). Seismic-Response-Controlled Structure with Active mass Driver System. Part1: Design, EESD, 20, 133-149.

Kobori, T., Koshika, N., Yamada, K. and Ikeda Y. (1991). Seismic-Response-Controlled Structure with Active Mass Driver System. Part2: Verification, EESD, 20, 151-166.

Sato, T. and Toki, K. (1990). Active Control of Seismic Response of Structures. Journal of Intelligent Material System and Structures, 1, No.4, 447-475

Sato, T., Toki, K., Mochizuki, T. and Yoshikawa, M. (1994). Optimal Closed-Open Loop Control Law for Seismic Response of Structures. Proc. of the 1st World Conf. on Structural Control, Los Angeles. TP2-12-21.

Toki, K., Sato, T., Yoshikawa, M., Kurimoto, M. and Inaba, K. (1994). Active Control of Seismic Response of a Structure by a Mass Driver System. Proc. of the World Conf. on Structural Control, Los Angeles, FP1-33-42.

Yang, J.N., Akbarpour, A. and Ghaemmaghami, P. (1987). New Optimal Control Algorithms for Structural Control. Journal of Engineering Mechanics, ASCE, 113, No.9, 1369-1386

Yang, J.N., Li, Z. and Liu, S.C. (1992). Stable Controller for Instantaneous Optimal Control, Journal of Engineering Mechanics, ASCE, 118, No.8, 1612-1630.